Holographic technique for measurement of the kinetic constant and optical modulation of photosensitive materials

L. F. Avila,[1,*] A. A. Freschi,[2] and Lucila Cescato[1]

[1]Optics Laboratory, Gleb Wataghin Institute of Physics, CxP 6165, University of Campinas (UNICAMP), 13083-970 Campinas, São Paulo, Brazil

[2]Centro de Engenharia, Modelagem e Ciências Sociais Aplicadas (CECS), Universidade Federal do ABC (UFABC), 09210-170 Santo André, São Paulo, Brazil

*Corresponding author: lfavila@ifi.unicamp.br

Received 15 March 2010; revised 17 May 2010; accepted 18 May 2010; posted 18 May 2010 (Doc. ID 125471); published 14 June 2010

We use a holographic technique to measure simultaneously and separately the temporal evolution of the refractive-index and the absorption coefficient modulations induced by light in a photosensitive material. The technique is phase sensitive, allowing separation of the signals from the phase and from the amplitude grating. The refractive-index and the absorption coefficient modulations as well as the kinetic constant of the photoreaction in the positive photoresist SC 1827 were measured at three different wavelengths. The results were compared with independent measurements, performed under homogeneous exposition. The good accord demonstrates the applicability of the technique to study photosensitive materials.

OCIS codes: 160.5335, 230.1950, 090.7330, 120.4530, 120.4120.

1. Introduction

Photosensitive materials are employed in a wide range of applications. They can be used to control light in glasses and windows [1], for photopolymerization of molds in dentistry [2] and in photolithographic processes of graphic and electronic industries [3], and for optical storage of images and information [4]. During the latter half of the 19th century many photosensitive materials were employed as optical memories: photographic emulsions [5], photopolymers [6], photorefractive crystals [7], and chalcogenide glasses [8]. In such materials, the local changes in the optical constants, induced by light, can be used for storage of information that can also be read by light.

To check the potential of a photosensitive material for optical memories it is necessary to characterize such changes by measurement of the maximum optical constant variations that can be induced by light, the spectral sensitivity of the material, the sensitivity to the light, the thermal and temporal stability, and the spatial resolution. The simplest way to characterize such changes is with the use of homogeneous exposure followed by measurement of the optical property. This method, however, requires the use of highly sensitive instruments to detect minor changes in the homogeneous optical constants of the material, and it does not allow the study of the spatial resolution of the material. To overcome this limitation, an interesting alternative is to expose the photosensitive material to a periodic light pattern (using a grating mask or an interference fringe pattern) instead of homogeneous light. In this case a periodic modulation of the optical constants will be recorded in the photosensitivity material that can be measured by diffraction [9]. This method allies the high sensitivity of the

0003-6935/10/183499-07$15.00/0

diffraction measurements [10] with the possibility to measure the spatial resolution [11].

In contrast, if the photosensitive material is exposed to a fringe pattern, a probe beam (that does not sensitize the material) can be used to measure and to follow the grating evolution. In this case dynamic changes in the material can be measured [12]. Another possibility is to measure the self-diffraction of the same interfering beams that generate the grating [13]. In this case, in each direction of the transmitted beams there is interference (wave mixing) between the zeroth transmitted beam and the first diffracted order of the other beam (Fig. 1). Such a signal is more sensitive than the direct diffraction efficiency measurement using a reference beam [13], and it is also phase sensitive [14]. The phase difference between the transmitted (zero-order) and the first-order diffracted beam depends on the phase perturbations [15] between the arms of the interferometer and on the nature of the photosensitive material [16].

The refractive-index changes induced by the fringe light pattern generate a phase grating in the photosensitive material whereas the absorption coefficient changes generate an amplitude grating. Within the limit of low modulation, the waves diffracted by the phase and by the amplitude grating are $\pi/2$ phase shifted between each other [17], generating uncoupled interference terms in the wave mixing between the zero-order transmitted beam and the first diffracted order of the other beam (Fig. 1). In two earlier papers [18,19], it was proposed to add and to subtract the wave mixing signals in these two symmetric directions of the interfering beams (Fig. 1) to separate the signals from the phase and from the amplitude grating. The same signals are also used for interferometer feedback to correct the fringe perturbations. Such a method [18,19] allows the simultaneous and independent measurement of the refractive index and of the absorption coefficient modulation; however, the temporal evolution measurement leads to different kinetic constant values (by approximately a factor of 2) of the photoreactions measured from the phase and from the amplitude gratings. Here we demonstrate a different method to process the self-diffraction signals to separate the phase and amplitude grating without introduction of systematic errors in the kinetic constant measurement. Different from the former method [18,19], the detection is now performed in a unique direction of the transmitted beams and the separation of the signals is performed by measuring the harmonics of the signal in this unique arm instead of the sum and subtraction of the signals in the two symmetric directions (arms). In addition to the possibility of simultaneous and independent measurement of the refractive index and the absorption coefficient modulation, this new method allows the measurement of kinetic constant values of photoreaction and the study of temporal evolution of photosensitive materials.

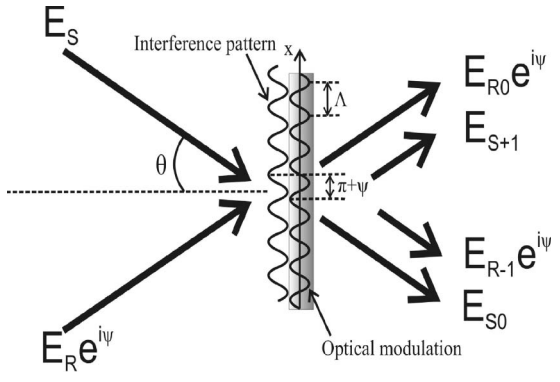

Fig. 1. Wave mixing. The interference pattern inside the photoresist film induces optical modulation. The phase in the incident E_R wave arises from phase perturbations between the arms of the interferometer.

2. Self-Diffraction

Consider two plane waves (E_R and E_S) with irradiances I_1 and I_2, respectively, interfering as shown in Fig. 1. The resulting interference light pattern can be described by

$$I = I_1 + I_2 + 2\sqrt{I_1 I_2}\cos\left(\frac{2\pi}{\Lambda}x\right). \tag{1}$$

With fringe period $\Lambda = \lambda/2\sin\theta$, θ is the half-angle formed between the incident beams and λ is the wavelength of the incident light. When a photosensitive material is exposed to this fringe pattern, the changes in the photosensitive material, induced by light, generate a cosinusoidal refractive-index modulation (phase grating) and a cosinusoidal absorption coefficient modulation (amplitude grating). For most photosensitive materials these modulations are in phase or in counterphase with the fringe pattern. These modulations diffract the incident beams that are generated in each direction of the transmitted waves, the interference between the zeroth transmitted order and the first diffracted order of the other beam. Assuming the presence of a phase perturbation (ψ) in the incident wave E_R that shifts the interference fringe pattern of the same phase (Fig. 1), behind the hologram, in direction R (Fig. 1), we will obtain the sum of the transmitted wave $E_{R0}\cdot e^{i\psi}$ and the diffracted wave E_{S+1}, with E_{S+1} being the first diffracted order of incident wave E_S. The analogy occurs in the direction of S. Thus the irradiance in each direction of incident waves R and S behind the hologram (Fig. 1) is given by

$$I_R = \frac{1}{2}\sqrt{\frac{\varepsilon_0}{\mu_0}}|E_{R0}e^{i\psi} + E_{S+1}|^2, \tag{2}$$

$$I_S = \frac{1}{2}\sqrt{\frac{\varepsilon_0}{\mu_0}}|E_{S0} + E_{R-1}e^{i\psi}|^2. \tag{3}$$

From the coupled wave theory [17] for a mixed phase and amplitude symmetrical grating at the Bragg

incidence within the limit of low modulation, the first diffracted order E_{R-1} (and, analogously, for E_{S+1}) is related to the incident wave by

$$E_{R-1} = D\left(\sqrt{\eta_A} + i\sqrt{\eta_P}\right)E_R. \tag{4}$$

Here, $\eta_A = (d\Delta\alpha/4\cos\theta)^2$ and $\eta_P = (\pi d\Delta n/2\lambda\cos\theta)^2$ represent the diffraction efficiency of the amplitude and the phase gratings, respectively, $\Delta\alpha$ and Δn represent the peak-to-peak absorption and refractive-index modulations, respectively, d is the film thickness, λ is the wavelength of the incident light, θ is the Bragg angle inside the material, $D = \exp(-\bar{\alpha}d/\cos\theta)$ is the average attenuation of the film, and $\bar{\alpha}$ is the average absorption coefficient. Note the presence of i in Eq. (4) that results from phase shift $\pi/2$ between the phase and the amplitude grating. Substituting Eq. (4) into Eq. (3) and E_{S+1} into Eq. (2) we obtain

$$I_R = I' + \beta\sqrt{\eta_A}\cos\psi + \beta\sqrt{\eta_P}\sin\psi, \tag{5}$$

$$I_S = I'' + \beta\sqrt{\eta_A}\cos\psi - \beta\sqrt{\eta_P}\sin\psi, \tag{6}$$

where I' and I'' are constants that depend on the light intensity and $\beta = 2D^2\sqrt{I_1 I_2}$. As can be seen in Eqs. (5) and (6), the term $\beta\sqrt{\eta_P}\sin\psi$ has opposite signals. Thus, by adding or subtracting the irradiance in both directions of the transmitted beams, the amplitude grating signal and the phase grating signal can be separated [18,19].

If we introduce a sinusoidal phase perturbation

$$\psi = \psi_d \sin\Omega t \tag{7}$$

of amplitude ψ_d and frequency Ω (much higher than the inverse of the response time of the photosensitive material) in one arm of the interferometer, periodic phase perturbation ψ generates in the transmitted beam harmonics of Ω in transmitted irradiances:

$$I_R = I_R^{\mathrm{dc}} + I_{R\Omega} + I_{R2\Omega} + \cdots, \tag{8}$$

where

$$I_R^{\mathrm{dc}} = I' + \beta[\sqrt{\eta_P}\sin(\psi) + \sqrt{\eta_A}\cos(\psi)]J_0(\psi_d), \tag{9}$$

$$I_{R\Omega} = 2J_1(\psi_d)\beta[\sqrt{\eta_P}\cos(\psi) - \sqrt{\eta_A}\sin(\psi)]\sin(\Omega t), \tag{10}$$

$$I_{R2\Omega} = 2J_2(\psi_d)\beta[\sqrt{\eta_P}\sin(\psi) + \sqrt{\eta_A}\cos(\psi)]\cos(2\Omega t). \tag{11}$$

These harmonics can be measured by a photodetector placed behind the photosensitive material in the region of the transmitted wave. The harmonics of the photodetector signal can be filtered through a lock-in amplifier. As can be seen from Eqs. (10) and (11), if there is no external phase perturbations ($\psi = 0 \Rightarrow \sin\psi = 0, \cos\psi = 1$), the amplitude of the first harmonic is proportional to the efficiency of the phase grating, whereas the amplitude of the second harmonic is proportional to the efficiency of the amplitude grating [20]. Thus by using two lock-in amplifier switches at the first and second harmonics, respectively, the signal from both gratings can be measured simultaneously and separately.

3. Experimental

To check the potential of this technique to study photosensitive materials we prepared films of the SC 1827 positive photoresist (Rohn & Hass, Croydon, Pennsylvania). The photoresist was coated on glass or quartz substrates by spin coating to form films approximately 4 μm thick. The thickness of each sample was measured after optical measurements were taken with a Sloan Dektak 3 ST profilometer.

A. Measurement Using Homogeneous Exposures

For comparison, we characterize the optical changes induced by light in the positive photoresist SC 1827 by performing homogeneous light exposure at three different laser wavelengths: λ = 325, 442, and 458 nm. To avoid interference problems, a rotating diffuser was used to expand the laser beam and to break its coherence. For the refractive-index measurements the samples were exposed to different doses of homogeneous light. After exposure the refractive index of each sample was measured using prism coupler Model 2010 (Metricon Corporation, Pennington, New Jersey).

To measure the absorption coefficient, the transmittance of each sample was exposed to a different wavelength and was measured during exposure. From these transmittance curves we can obtain absorption coefficient (α) by

$$T = (1-R_1)(1-R_2)(1-R_3)e^{-2\alpha d}, \tag{12}$$

where R_1, R_2, and R_3 are, respectively, the air photoresist, photoresist substrate, and substrate–air interface reflectance.

B. Measurement Using Holographic Exposures

The holographic exposures were performed using two similar interferometers (whose setup is schematically shown in Fig. 2): one for the visible ($\lambda = 458$ nm) and the other provided with UV optics for wavelengths $\lambda = 442$ and 325 nm. The scheme of the interferometers used in our experiment is shown in Fig. 2. A laser beam is split into two beams that are expanded and collimated and again superimposed. The fringe period depends on the laser wavelength and on the half-angle between the interfering beams. In our experiments we changed the interfering angle to keep constant the fringe period of 1 μm for each laser wavelength. The photosensitive material (sample) is placed at the superimposition region.

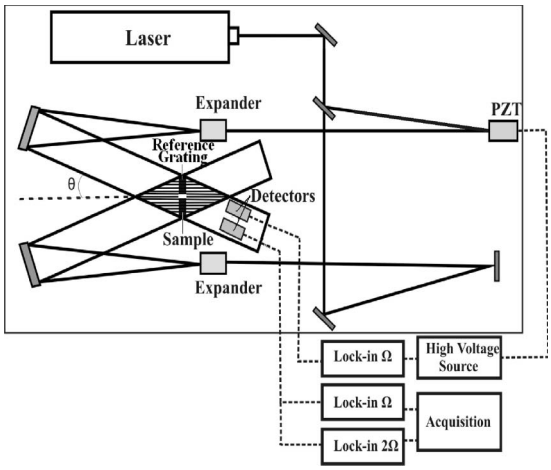

Fig. 2. Experimental setup.

C. Fringe Locker System

To eliminate the fringe perturbations (ψ) during recording, we used a reference phase grating. The reference grating was generated by exposing a photoresist film to the same interference pattern. After development of the photoresist a relief modulation (phase grating) appears. For angular repositioning of the reference grating in the interference fringe pattern we maximize the moirélike pattern (Fig. 3) formed by the interference between the transmitted wave and the wave diffracted at the reference grating. A photodetector, positioned behind the reference grating, can be connected to a lock-in amplifier and used to detect and to correct the fringe perturbations (ψ). For a reference phase grating, the amplitude grating [η_A of Eq. (10)] can be neglected and the amplitude of the first harmonic signal [Eq. (10)] can be measured with a lock-in amplifier and used as system feedback until it reaches equilibrium when the feedback signal vanishes. In this situation, $\cos\psi = 0$ in Eq. (10), which corresponds to either a bright or a dark fringe [Fig. 3(b)] at the detector [from Eq. (9)] [14]. Although the fringe pattern remains locked at the small detector area, outside this region thermal perturbations can produce distortions in the fringe pattern.

D. Self-Diffraction Measurement

To characterize a photosensitive material we placed the photosensitive sample in the same interference fringe pattern (as shown in Fig. 2), as close to the reference grating as possible. A second photodetector is placed behind the sample of photosensitive material (Fig. 2). This photodetector is connected simultaneously to two lock-in amplifiers (Fig. 2), switched at the first and second harmonics. If we assume that $\psi = 0$ (because of the fringe locker system), voltage signals V_Ω and $V_{2\Omega}$, measured with the lock-in amplifiers that are connected to the photodetector, are, respectively, proportional to the irradiance harmonics described by Eqs. (10) and (11):

$$V_\Omega = KJ_1(\psi_d)\sqrt{\eta_P}, \tag{13}$$

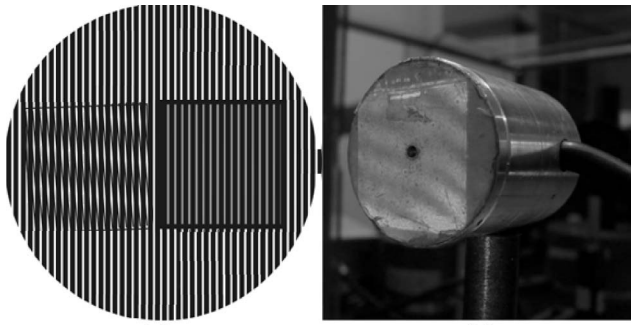

Fig. 3. (a) Scheme of an interference pattern incident over the reference grating (left) and the photosensitive material (right). The reference grating was recorded, developed, and repositioned in the same place with the material. Misalignment between the interference fringe and the recorded grating produces a moiré interference pattern. (b) Moirélike pattern projected on the detector.

$$V_{2\Omega} = KJ_2(\psi_d)\sqrt{\eta_A}. \tag{14}$$

By substituting diffraction efficiencies η_P and η_A given by [17] into Eqs. (12) and (13), from these signals we can obtain the coefficient of absorption modulation ($\Delta\alpha$) and the refractive-index modulation (Δn), respectively,

$$\Delta n = \frac{\lambda\cos\theta}{2\pi d J_1(\psi_d)}\frac{\sqrt{I_1 I_2}}{I_1}\frac{V_\Omega(t)}{V_D(t)}, \tag{15}$$

$$\Delta\alpha = \frac{\cos\theta}{dJ_2(\psi_d)}\frac{\sqrt{I_1 I_2}}{I_1}\frac{V_{2\Omega}(t)}{V_D(t)}, \tag{16}$$

where V_D is the dc detector voltage, d is the film thickness, λ is the light wavelength, θ is the Bragg angle inside the material, I_1 and I_2 represent the intensity of the incident beams, and V_Ω and $V_{2\Omega}$ are the voltages measured by the lock-in amplifiers switched at the first and second harmonics, respectively.

4. Results

For both types of measurement (homogeneous and holographic exposures) we consider the time of exposure multiplied by the average light intensity inside the film. This average intensity ($\bar{I}$) takes into account the average light absorption at each wavelength inside the photoresist film by

$$\begin{aligned}\bar{I} &= (1 - R(\theta_0))\frac{I_0}{d}\int_0^d e^{-2\bar{\alpha}z}\mathrm{d}z \\ &= (1 - R(\theta_0))\frac{I_0}{2\bar{\alpha}d}(1 - e^{-2\bar{\alpha}d}),\end{aligned} \tag{17}$$

where d is the film thickness, $\bar{\alpha}$ is the average absorption coefficient, I_0 is the irradiance at the first interface of the photoresist film, and $R(\theta_0)$ is the reflectance for incident angle θ_0.

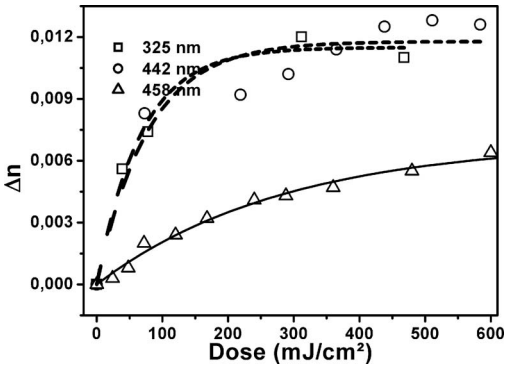

Fig. 4. Refractive-index modulations under homogeneous laser exposure for three different wavelengths. The refractive-index measurements were taken with a Metricon prism coupler at $\lambda = 633\,\text{nm}$.

A. Homogeneous Exposures

Figure 4 shows the refractive-index changes of samples exposed to different doses at laser wavelengths of $\lambda = 325$, 442, and 458 nm. The measurements were performed at $\lambda = 633\,\text{nm}$, as described in Subsection 3.A. Figure 5 shows the absorption coefficient changes as a function of exposure to the same laser wavelengths of $\lambda = 325$, 442, and 458 nm, as described in Subsection 3.A. In this case the measurement is at the same wavelength as the exposure.

Assuming that the optical changes are caused by a single photoreaction [21], both the refractive-index modulation and the absorption coefficient modulation should be related to the exposure by [21,22]

$$\Delta n = \Delta n_{\max}(1 - e^{-\text{CE}}), \tag{18}$$

$$\Delta \alpha = \Delta \alpha_{\max}(1 - e^{-\text{CE}}). \tag{19}$$

Fitting the experimental data to Eqs. (18) and (19) is shown in Figs. 4 and 5, respectively. From these fittings we obtain the maximum modulations ($\Delta\alpha_{\max}$ and $\Delta n_{\max}$) as well as the kinetic constant of the photoreaction (C) for each wavelength of exposure. This kinetic constant is known in the literature as Dill parameter C [23]; the $\Delta\alpha_{\max}$ is known as Dill parameter A [22,23]. The maximum modulation values $\Delta n_{\max}$ and $\Delta\alpha_{\max}$ as well as the values of C are listed in Table 1 for the three exposure wavelengths of λ = 325, 442, and 459 nm.

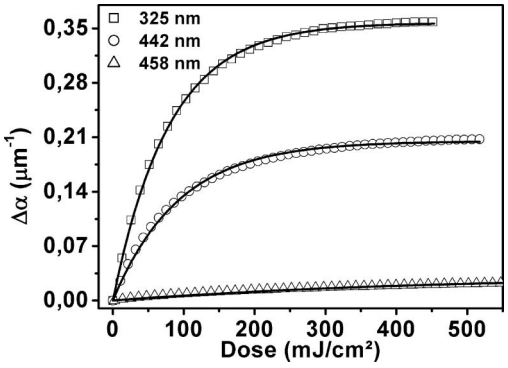

Fig. 5. Absorption coefficient modulations under homogeneous laser exposure for three different wavelengths. The measurements were taken in real time.

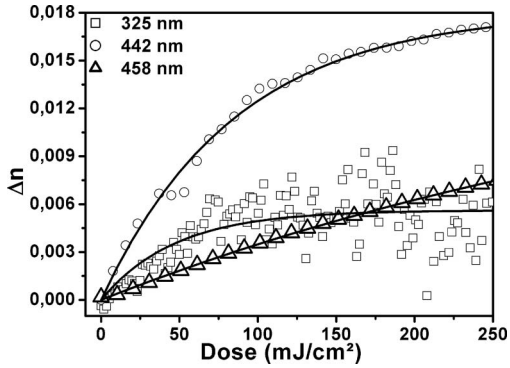

Fig. 6. Real-time holographic measurements of the refractive-index modulation for three different wavelengths.

B. Holographic Exposures

Using the method described in Subsection 3.B. we measured the refractive-index modulation and the absorption coefficient modulation as a function of light exposure. Figure 6 shows the results for the measurement of the index modulations as a function of light exposure for the three different wavelengths of $\lambda = 325$, 442, and 458 nm. Note that the exposure of light in this case corresponds to the peak-to-peak fringe pattern given by Eq. (1).

The refractive-index modulation saturates for light exposure of approximately $2\,\text{J/cm}^2$. Note that the refractive-index modulation saturates at the value of approximately $\Delta n = 3 \times 10^{-3}$. Figure 7 shows the same for absorption coefficient modulation $\Delta\alpha$.

Note that, for wavelength $\lambda = 325\,\text{nm}$, the diffraction efficiency of the amplitude grating ($\eta_A \sim 1.2\%$) is much greater than the diffraction efficiency of the phase grating ($\eta_P \sim 0.04\%$). Thus small uncorrected phase perturbations (ψ) [in Eq. (10)] are amplified, increasing the noise in the refractive-index measurement, as can be seen in Fig. 6. For wavelength $\lambda = 458\,\text{nm}$, the opposite occurs: the diffraction efficiency of the amplitude grating ($\eta_A \sim 0.01\%$) is much smaller than the diffraction efficiency of the phase grating ($\eta_P \sim 0.2\%$) in Eq. (11). Thus, for this

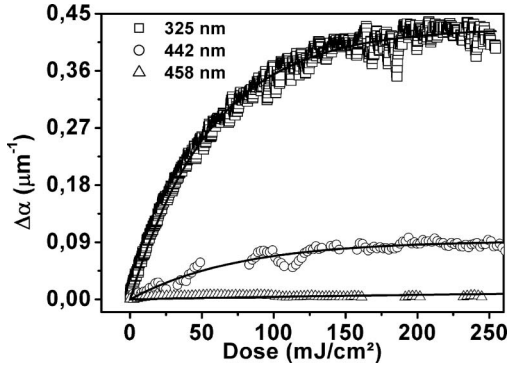

Fig. 7. Real-time holographic measurements of the absorption coefficient modulations for three different wavelengths.

Table 1. Kinetic Constant for Different Exposures and for Independent Measurement Methods

Wavelength (nm)	Method	Δn_{max}	$\Delta\alpha_{max}(\mu m^{-1})$	$C_{\Delta n}(cm^2/mJ)$	$C_{\Delta\alpha}(cm^2/mJ)$
325	Holographic	0.005	0.43	0.021	0.018
	Homogeneous	0.001*	0.36	0.015	0.013
442	Holographic	0.018	0.18	0.012	0.013
	Homogeneous	0.012*	0.21	0.014	0.011
458	Holographic	0.017	0.018	0.0022	0.0024
	Homogeneous	0.007*	0.032	0.0028	0.0022

wavelength the noise is amplified for the holographic measurement of the absorption coefficient (Fig. 7). The noise in the $\Delta\alpha$ measurement in Fig. 7 (for $\lambda = 458\,nm$) is not so clear as in Fig. 6 ($\lambda = 325\,nm$) because of the scale.

Thus, by fitting the experimental data of Figs. 4 and 5 into Eqs. (18) and (19) we can also obtain the maximum modulations ($\Delta\alpha_{max}$ and Δn_{max}) as well as the kinetic constant of photoreaction C for each exposure wavelength. These values are shown in Table 1.

5. Discussion and Conclusion

By comparing the values of the kinetic constants (C) in Table 1, for each wavelength of exposure, we observed good agreement between both holographic measurements from the refractive-index grating and from the absorption coefficient grating, confirming that the method is free from systematic error. We also observed good agreement of the kinetic constant between the holographic and the homogeneous exposure measurements for both the refractive index and the absorption coefficient. By performing an average, for $\lambda = 325\,nm$ we found a mean kinetic constant of $C = 0,017 \pm 0.003\,(cm^2/mJ)$, for $\lambda = 442\,nm$, $C = 0,012 \pm 0.001\,(cm^2/mJ)$, and for $\lambda = 458\,nm$, $C = 0,0024 \pm 0.0002\,(cm^2/mJ)$. As can be seen, kinetic constant C decreases when the wavelength increases, indicating that the quantum efficiency of the photoreaction in photoresist SC 1827 decreases when the wavelength increases [23].

We also observed good agreement between the holographic and the homogeneous measurement of the maximum modulation of the absorption coefficient ($\Delta\alpha_{max}$) for $\lambda = 325\,nm$ the $(\Delta\alpha_{max}) = 0.40 \pm 0.04\,\mu m^{-1}$ and for $\lambda = 442\,nm$ the $(\Delta\alpha_{max}) = 0.20 \pm 0.02\,\mu m^{-1}$. For $\lambda = 458\,nm$ the values of the maximum absorption coefficient modulation obtained from the holographic measurements are less than that corresponding to homogeneous exposures. For this wavelength the holographic measurements of $\Delta\alpha$ present high noise because, as explained in Subsection 4.B, the diffraction efficiency of the amplitude grating (η_A) is much smaller than the diffraction efficiency of the phase grating (η_P).

The maximum absorption coefficient modulation ($\Delta\alpha_{max}$), however, also decreases with the increase in wavelength. This behavior corresponds to the decrease in quantum efficiency for higher wavelengths that also reduces the kinetic constant of the photoreaction.

The maximum refractive-index modulation (Δn_{max}) measured under homogeneous illumination (indicated by an asterisk in Table 1) was performed at $\lambda = 633\,nm$. Thus these values should be smaller than those measured at shorter wavelengths. For these curves the refractive-index modulation is approximately the same ($\Delta n_{max} = 0.012$) for $\lambda = 325\,nm$ and $\lambda = 442\,nm$ and smaller ($\Delta n_{max} = 0,007$) for $\lambda = 458\,nm$. This decrease in Δn_{max} is also compatible with the decrease in the quantum efficiency with the increase in wavelength. For holographic measurements, however, the maximum refractive-index modulation (Δn_{max}) for the exposure wavelength of $\lambda = 325\,nm$ is much less than that expected using homogeneous exposures, as well as in comparison with the (Δn_{max}) obtained for the larger exposure wavelengths under holographic exposure. As can be seen in Fig. 6, for this wavelength we observe strong noise in the holographic measurement of (Δn_{max}) because now the diffraction efficiency of the phase grating (η_P) is much less than the diffraction efficiency of the amplitude grating (η_A), as explained in Subsection 4.B.

In conclusion, our results demonstrate the applicability of this holographic technique to study the kinetic constant of photosensitive materials as well as to measure separately the absolute values of the absorption coefficient modulation and refractive-index modulation. The limitation of the technique is the noise caused by a large difference between diffractive signals of the phase and amplitude gratings as it occurs in the SC1827 positive photoresist for the Δn measurement at $\lambda = 325\,nm$ and for the $\Delta\alpha$ measurement at $\lambda = 458\,nm$.

We acknowledge Fundação de Amparo à Pesquisa do Estado de São Paulo (FAPESP), Fotônica para Comunicações Ópticas (FOTONICOM), and Conselho Nacional de Desenvolvimento Científico e Tecnológico (CNPq) for financial support of this work.

References

1. G. K. Megla, "Optical properties and applications of photochromic glass," Appl. Opt. **5**, 945–960 (1966).
2. L. G. Lovell, H. Lu, J. E. Elliott, J. W. Stansbury, and C. N. Bowman, "The effect of cure rate on the mechanical properties of dental resins," Dent. Mater. **17**, 504–511 (2001).
3. E. Reichmanis, F. M. Houlihan, O. Nalamasu , and T. X. Neenan, "Chemical amplification mechanisms for microlithography," Chem. Mater. **3**, 394–407 (1991).

4. A. V. Kolobov and J. Tominaga, "Chalcogenide glasses as prospective materials for optical memories and optical data storage," J. Mater. Sci. Mater. Electron. **14**, 677–680 (2003).
5. B. H. Carroll and D. Hubbard, "The photographic emulsion. I. The comparison of emulsions made with different bromides," J. Phys. Chem. **31**, 906–921 (1927).
6. L. Dhar, K. Curtis, M. Tackitt, M. Schilling, S. Campbell, W. Wilson, A. Hill, C. Boyd, N. Levinos, and A. Harris, "Holographic storage of multiple high-capacity digital data pages in thick photopolymer systems," Opt. Lett. **23**, 1710–1712 (1998).
7. D. Psaltis, F. Mok, and H.-Y. S.Li, "Nonvolatile storage in photorefractive crystals," Opt. Lett. **19**, 210–212 (1994).
8. A. Zakery and S. R. Elliott, "Optical properties and applications of chalcogenide glasses: a review," J. Non-Cryst. Solids **330**, 1–12 (2003).
9. G. F. Mendes, L. Cescato, and J. Frejlich, "Gratings for metrology and process control. 1: a simple parameter optimization problem," Appl. Opt. **23**, 571–575 (1984).
10. J. Frejlich and L. Cescato, "Analysis of a phase-modulating recording mechanism in negative photoresist," J. Opt. Soc. Am. **71**, 873–878 (1981).
11. M. S. Sthel, C. R. A. Lima, and L. Cescato, "Photoresist resolution measurement during the exposure process," Appl. Opt. **30**, 5152–5156 (1991).
12. P. Cheben and M. L. Calvo, "A photopolymerizable glass with diffraction efficiency near 100% for holographic storage," Appl. Phys. Lett. **78**, 1490–1492 (2001).
13. L. Cescato and J. Frejlich, "Self-diffraction for intrinsic optical modulation evolution measurement in photoresists," Appl. Opt. **27**, 1984–1987 (1988).
14. L. Cescato and J. Frejlich, "Self stabilized real time holographic recording," in *Three-Dimensional Holographic Imaging*, C. J. Kuo and M. H. Tsai, eds. (Wiley, 2002), pp. 21–46.
15. J. Frejlich, L. Cescato, and G. F. Mendes, "Analysis of an active stabilization system for a holographic setup," Appl. Opt. **27**, 1967–1976 (1988).
16. P. M. Garcia, L. Cescato, and J. Frejlich, "Phase-shift measurement in photorefractive holographic recording," J. Appl. Phys. **66**, 47–49 (1989).
17. H. Kogelnik, "Coupled wave theory for thick hologram gratings," Bell Syst. Tech. J. **48**, 2909–2947 (1969).
18. J. Frejlich, A. A. Kamshilin, and P. M. Garcia, "Selective two-wave mixing in photorefractive crystals," Opt. Lett. **17**, 249–251 (1992).
19. C. M. B. Cordeiro, A. A. Freschi, and L. Cescato, "Progress on holographic techniques to measure real-time phase and amplitude gratings in photosensitive materials," J. Opt. A: Pure Appl. Opt. **5**, S170–S174 (2003).
20. J. Pinsl, M. Gehrtz, and C. Bräuchle, "Phase-modulated holography: a new technique for investigation of solid state photochemistry and hologram formation mechanisms," J. Phys. Chem. **90**, 6754–6756 (1986).
21. L. F. Avila and C. R. A. Lima, "Dill's parameter measure in liquid photosensitive materials via interferometric method," Eur. Polym. J. **43**, 2041–2045 (2007).
22. C. A. Mack, "Absorption and exposure in positive photoresist," Appl. Opt. **27**, 4913–4919 (1988).
23. F. H. Dill, W. P. Hornberger, P. S. Hauge, and J. M. Shaw, "Characterization of positive photoresist," IEEE Trans. Electron. Devices **22**, 445–452 (1975).